Ultrafast Studies on the Photophysics of Matrix-Isolated Radical Cations of Polycyclic Aromatic Hydrocarbons

Liang Zhao,[†] Rui Lian,[‡] Ilya A. Shkrob,[‡] Robert A. Crowell,*[,‡] Stanislas Pommeret,[‡,§] Eric L. Chronister,[†] An Dong Liu,[‡,||] and Alexander D. Trifunac[‡]

Chemistry Department, University of California at Riverside, Riverside, California 92521, Chemistry Division, Argonne National Laboratory, Argonne, Illinois 60439, and CEA/Saclay, DSM/DRECAM/SCM/URA 331 CNRS 91191 Gif-Sur-Yvette Cedex, France

Received: August 7, 2002; In Final Form: July 30, 2003

Ultrafast relaxation dynamics for photoexcited PAH cations isolated in boric acid glass have been studied using femtosecond and picosecond transient grating spectroscopy. With the exception of perylene$^+$, the recovery kinetics for the ground doublet (D_0) states of these radical cations are biexponential, containing fast (<200 fs) and slow (3−20 ps) components. No temperature dependence or isotope effect was observed for the fast component, whereas the slow component exhibits both the H/D isotope effect (1.1−1.3) and a strong temperature dependence (15 to 300 K). We suggest that the fast component is due to internal D_n to D_0 conversion and that the slow component is due to vibrational energy transfer (VET) from a hot D_0 state to the glass matrix. The observed rapid, efficient deactivation of the photoexcited PAH cations accounts for their remarkable photostability and has important implications for astrochemistry because these cations are the leading candidates for the species responsible for the diffuse interstellar bands (DIB) observed throughout the galaxy.

1. Introduction

Processes involving radical cations of polycyclic aromatic hydrocarbons (PAHs) occur in many areas of chemistry such as organic synthesis, photo- and radiation chemistry, and astrochemistry. In particular, these radical cations are thought to be responsible for diffuse interstellar bands (DIBs) in star-forming clouds in our galaxy.[1−4] Although the association of these ubiquitous bands with the PAH cations is still tentative,[1] these radical cations, together with their parent molecules and corresponding carbonium ions, could be the prevalent form of the organic matter in the universe.[4] Why are these exotic, by terrestrial standards, species so common? Some researchers speculate that the PAHs are generated in mass-losing carbon stars, in ion−molecule reactions of neutral and ionized C atoms, by the condensation of C chains, or by the thermo- and photoinduced condensation of molecules adsorbed on dust particles. (See, for example, ref 4.) In these scenarios, the high abundance of the PAH cations is due to the high production rate of their parent molecules. Other researchers focus[1,3,5] on the dynamics of the gas-phase carbonaceous molecules and ions in the interstellar medium where these species are exposed to intense radiation from young stars. It seems that PAH cations of intermediate size are favored in this harsh environment.[3,5] Regardless of the exact answer, it is certain that (i) PAH cations are products of lengthy chemical evolution driven by heat and radiation and (ii) these cations are abundant in space because they are more photostable than most neutral molecules and anions.[1−4] In particular, the primary decay processes for photoexcited radical cations of PAHs are nonradiative: [5−10] almost all of the excitation energy is converted into heat that (in the interstellar medium) is emitted as IR radiation.[1,2] It is the purpose of this work to study the photophysical processes of PAHs.

Although the photophysics and reactivity of the excited singlet and triplet states of neutral PAH molecules are well understood, very little is known about the photophysics of their radical cations. In the gas phase, $-H$, $-H_2$, and $-C_2H_2$ photofragmentation of $C_{10}-C_{16}$ PAH cations have been studied by mass spectrometry. [5] Typical dissociation rates for 7-eV excess energy are $(1-3) \times 10^3$ s^{-1}, and the onsets of dissociation are 4−4.5 eV (which is close to the C−H bond dissociation energy). [5] These gas-phase studies demonstrate the remarkable photostability of PAH cations (as compared to that of their parent molecules) and suggest fast energy relaxation in these species. There have also been numerous EPR, UV−vis, and IR studies of matrix-isolated PAH cations. From these studies and concurrent ab initio and density functional theory calculations, a wealth of data on the structure and energetics of aromatic radical cations has emerged (e.g., see Table 1 and references given therein).

Recently, Vauthey and co-workers [7,8] examined the relaxation dynamics of photoexcited matrix-isolated radical cations of several organic molecules, including perylene$^+$ and tetracene$^+$. The 640-nm ($D_0 \leftarrow D_1$) band in the fluorescence spectrum of perylene$^+$ was observed, and a quantum yield of 10^{-6} was obtained. Picosecond (for perylene$^+$) and subpicosecond (for tetracene$^+$) transient grating (TG) spectroscopy was used to observe the recovery of the D_0 state following laser photoexcitation (in the $D_0 \rightarrow D_5$ and $D_0 \rightarrow D_1$ bands, respectively). This study brought an unexpected result: although the $D_1 \rightarrow D_0$ conversion in tetracene$^+$ and perylene$^+$ was fast (25 to 100 ps, depending on the matrix)[7,8] as compared to the typical times

* To whom correspondence should be addressed. E-mail: rob_crowell@anl.gov. Tel. 630-2528089. Fax: 630-2524993.
[†] University of California at Riverside.
[‡] Argonne National Laboratory.
[§] CNRS.
[||] Permanent address: Institute of Low Energy Nuclear Physics, Beijing Normal University, Beijing, China.

10.1021/jp021832h CCC: $27.50
Published on Web 12/04/2003

TABLE 1: Energetics of the PAH Cations[a]

aromatic cation	D_0[b]	band excited[c]	energy of band excited, nm (ev)	symmetry of state excited	D_1	$E(D_1) - E(D_0)$, eV[c]	$E(D_1) - E(D_0)$, eV[d]
biphenyl$^+$	$^2B_{2g}$	D_3	680 (1.82)	$^2B_{3u}$	^2A_u	0.7[17b] 0.88[17a]	1.53[17e] (*0.0062*)
naphthalene$^+$	^2A_u	D_2	680 (1.82)	$^2B_{2g}$	$^2B_{1u}$	0.78[17a] 0.72[30]	0.894[16]
anthracene$^+$	$^2B_{2g}$	D_2	720 (1.72)	^2A_u	$^2B_{3g}$	1.13[30]	1.33[16]
pyrene$^+$	$^2B_{3g}$	D_5		^2A_u	$^2B_{2g}$	0.85[29]	0.85[29] 1.17[16]
perylene$^+$	^2A_u	D_5	540 (2.3)	$^2B_{3g}$	$^2B_{3g}$	1.56[16]	1.596 (*0.0068*)[16]

[a] Computation methods are LNDO/S + PERT CI (ref 17e), HMO (ref 17b), QCFF/PI + CI (ref 16), and CIPSI/PPP and CIPSI/PI + CI (ref 29). [b] The ground state, assuming D_{2h} symmetry. For ground-state biphenyl$^+$, D_2 symmetry with a torsion angle of ~20−40° between the aromatic rings is more appropriate.[17] [c] Relative energy of the first excited state as determined by photoelectron spectroscopy. [d] The same, by theoretical calculation. (In parentheses, the oscillator strength of the allowed $D_0 \rightarrow D_1$ transitions is indicated). [e] The same, from the onset of the 0−0 $D_0 \rightarrow D_1$ transition.

of $10^{-9}-10^{-6}$ s for the $S_1 \rightarrow S_0$ transition in neutral PAH molecules, [9] this conversion was much slower than the typical times of 10−500 fs for nonradiative $S_n \rightarrow S_{n-1}$ transitions that involve higher excited singlet states (S_n) of these PAH molecules. [9,10] Because the rate of nonradiative transition broadly correlates with the energy gap between the initial and final states, [10] these energetic S_n states should have provided a good reference system for the lower doublet states of aromatic radical cations because the corresponding energy gaps are comparable (0.5−1 eV; see Table 1). Because tetracene$^+$ and perylene$^+$ have unusually large D_1-D_0 gaps of 1.44 and 1.56 eV, [8] respectively, it appears that these two radical cations might represent the exception rather than the rule. To observe nonradiative transitions in a typical PAH cation, time resolution better than 1 ps is needed.

In this work, the photophysics of radical cations of perprotio and perdeuterio anthracene, naphthalene, biphenyl, and perylene stabilized in boric acid glass are studied using femtosecond transient grating spectroscopy. Our results suggest that for most of the PAH cations the excited electronic states relax through a nonradiative $D_n \rightarrow D_0$ transition that occurs in less than 200 fs. This process rapidly converts the electronic energy into vibrational energy of the ground D_0 state, which then undergoes vibrational energy transfer (VET) on a picosecond time scale by heat transfer to the matrix. The typical VET times observed in the boric acid glass are 5 to 20 ps. Perylene$^+$ has an exceptionally long lifetime for the $D_1 \rightarrow D_0$ conversion, ca. 19 ps, by virtue of its unusual energetics. To save space, some data are given in the Supporting Information. Figures and Tables with a designator "S" after the number (e.g., Figure 1S) are placed therein.

2. Experimental Section

Sample Preparation. Orthoboric acid (H_3BO_3), biphenyl-h_{10} and -d_{10}, naphthalene-h_8 and -d_8, anthracene-h_{10} and -d_{10}, pyrene-h_{10}, and perylene-h_{12} (see Figure 1S for the structure) of the highest purity available from Sigma-Aldrich were used as received. PAH-doped glass was prepared by adding crystalline PAHs to the boric acid melt at 200−240 °C. The melt was cast between two thin windows made of fused silica, calcium fluoride, or sapphire and produced high-quality, optically clear glasses upon cooling. The typical glass film thickness was 100 to 400 μm. These samples were then exposed to 5 to 50 pulses of 248-nm light (15 ns fwhm, 0.05 J/cm^2) from a Lambda Physik model LPx-120i KrF excimer laser at room temperature. Absorption spectra[11,12] confirmed the formation of radical cations[11] with conversion efficiency better than 80%. The concentrations of the radical cations were spectrophotometrically determined to be 0.1−0.5 mM (for perylene$^+$, ca. 20 μM). Because of a large nonresonant TG signal observed in the windows, the glass film was removed from the substrate, and transparent 2 mm × 2 mm pieces were mounted on the cold finger of a closed-cycle helium refrigerator (Lake Shore Cryogenics) operable from 10 to 300 K. [13] The typical absorbance of these films at the excitation wavelength was 0.3−1. For absorbances <0.1, the nonresonant TG signal from the glass matrix was superimposed on the TG signal from PAH cations.

Transient Grating Spectroscopy. The ground-state recovery dynamics of PAH cations were studied using femtosecond TG spectroscopy. Details of this technique can be found elsewhere.[7,8,14] Briefly, a standard three-beam transient grating setup using a folded BOXCARS geometry with crossing angles of ca. 2° was used.[7,8,14] Calcite Glan-Thomson polarizers were placed in each of the three beam paths and the scattered probe beam to ensure pure and parallel polarization so that the observed signal reflected the dynamics of the $\chi^{(3)}_{1111}$ element of the third-order nonlinear susceptibility tensor.[7,14] Under the conditions of our experiments, a density grating (due to the heat-induced expansion of the sample) is produced simultaneously with respect to the population grating that we are interested in observing. The density grating generates an acoustic standing wave that over time will affect the population grating. The density grating has no effect on our measurements because the small-angle geometry used in this setup (~2°) results in an acoustic period of >10 ns. The instrument response was determined by obtaining a nonresonant TG signal due to optical-field-induced electronic and nuclear Kerr effects in a thin plate of fused silica or undoped boric acid glass before and after each measurement. This response was Gaussian, with a typical fwhm of 60−70 fs (for femtosecond kinetics) or 160 fs (for picosecond kinetics).

The tunable source of femtosecond light pulses used in the experiments is an optical parametric amplifier (Spectra Physics OPA model 8000CF). The OPA is pumped by a 800-μJ, 800-nm, 55-fs fwhm pulse split off from a two-stage Ti:sapphire-based chirped pulse amplifier system (3.5 mJ) operated at a repetition rate of 1 kHz. Passing the output of the OPA through a pair of SF-10 prisms resulted in transform-limited pulses of 45−55 fs duration (depending on the wavelength). The pump

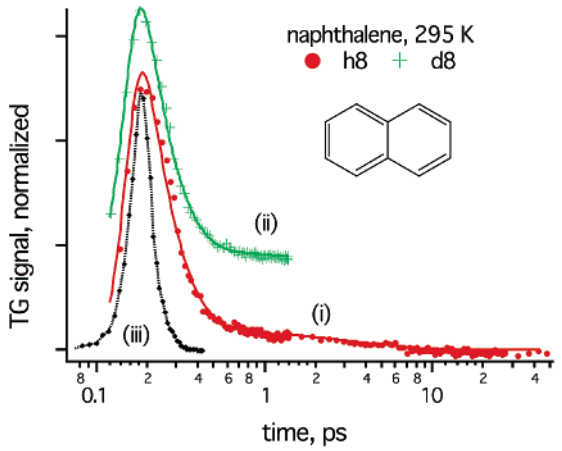

Figure 1. Transient grating signal for the recovery of the ground D_0 state of the radical cation observed in a 680-nm pump−680-nm probe ($D_0 \rightarrow D_2$ band, 0−0 transition) photoexcitation of naphthalene-h_8^+ (trace i, filled circles) and naphthalene-d_8^+ (trace ii, crosses) in a boric acid glass at 295 K. The optical density of this 300-μm-thick glass sample was ca. 1. The dashed line (trace iii, filled diamonds) is a nonresonant optical Kerr effect signal from a thin Suprasil plate, which is taken as an autocorrelation trace for the excitation/probe pulse (in this case, a Gaussian pulse of 63 fs fwhm). The solid line in trace i is the least-squares fit obtained by convoluting trace ii with a biexponential function. (The time constants are given in Table 2.) The fast component (<1 ps) is from the electronic deactivation of the D_1 state, and the slow component (1−20 ps, ca. 10% of the fast component in weight) is from the vibrational relaxation of a hot D_0 state. Trace ii is shifted upward for clarity. The solid line drawn through the crosses is the same curve as in trace i (i.e., there is no H/D isotope effect; see also Figure 3Sa in the Supporting Information).

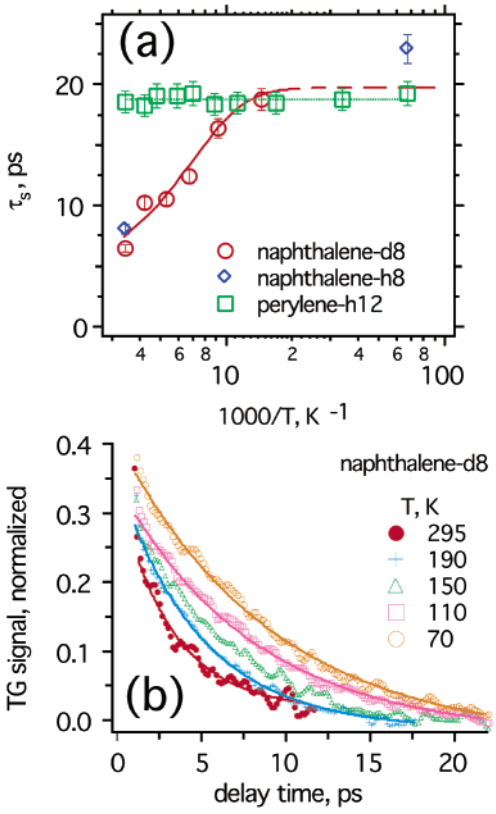

Figure 2. (a) Temperature dependencies of the time constant τ_s of the slow component for naphthalene-d_8^+ (open circles) and perylene-h_{12}^+ (open squares). Two data points (15 and 295 K) for naphthalene-h_8^+ (open diamonds) are also shown. The error bars give the standard deviation. The temperature dependence (70 to 300 K) of τ_s for naphthalene-d_8^+ can be fit using the empirical equation $1/\tau_s = k_0 + k_1 \exp(-E_a/RT)$, where $1/k_0 = 19.7$ ps, $1/k_1 = 3.5$ ps, and the activation energy $E_a = 31 \pm 8$ meV. The dashed section is a low-temperature extrapolation. (b) Slow-decay kinetics for the TG signal in the 680-nm pump−680-nm probe excitation of naphthalene-d_8^+ in boric acid glass. Both of these pulses were 160 fs fwhm. The sample temperatures are 295 K (filled circles), 190 K (crosses), 150 K (open triangles), 110 K (open squares), and 70 K (open circles). The lines drawn through the symbols are the least-squares exponential fits. The TG kinetics were normalized at the signal maximum (taken as unity). The initial "spike" (see Figure 1, traces i and ii) is not shown. As the temperature decreases, the relative weight of the slow component increases, and its decay kinetics become slower.

energy (in each pump beam) was less than 500 nJ, and the probe energy was less than 50 nJ. To subtract the background signal, one of the pump beams was chopped at 500 Hz, and the photodiode signal was fed into a digital lock-in amplifier (SRS model 810). Otherwise, the detection electronics were identical to those described previously. [15] To obtain subpicosecond kinetics, 50−100 traces acquired with a time constant of 30 ms were averaged. The delay times of the probe pulses were changed either linearly ($\Delta t = 15$ fs) or on a quasilogarithmic grid (Figure 1). [15] The error bars shown in some kinetics are 95% confidence limits. To obtain picosecond kinetics, the delay time of a 160-fs pulse was changed in steps of 150−200 fs, and 20−30 traces acquired with a time constant of 300 ms were averaged.

3. Results

Figure 1 shows a TG signal observed for the radical cation of naphthalene-h_8 in a UV-irradiated boric acid glass at 300 K. Only naphthalene$^+$ absorbs 680-nm light in this sample. The kinetics were obtained using 680-nm pump and probe pulses of 63 fs fwhm. The pump energy (1.82 eV) corresponds to the excitation of a strongly allowed $D_0 \rightarrow D_2$ transition (Figure 2S and Table 1). Following the excitation pulse, the recovery of the photobleached D_0 state is observed. The intensity of the grating signal is proportional to the square of the concentration of photoexcited cations. For an exponential process, the TG signal decays at twice the rate of the D_0 state recovery. Note that only the population grating[7,14] contributes to the TG signal observed at the end of the pump pulse. During photoexcitation, a nonresonant signal due to the optical Kerr effect (Figure 1)[8,14] contributes to the TG signal. This signal makes it difficult to observe rapid processes that occur in less than 50 fs.

Following the 680-nm photoexcitation of naphthalene$^+$, there is a short-lived TG signal whose single-exponential decay kinetics correspond to a lifetime τ_f of 195 ± 5 fs (Figures 1 and 3Sa). After the decay of this short-lived signal, there is a slower TG signal that decays over a time period of tens of picoseconds (Figures 1, 2b, and 3Sb). This slow signal comprises ca. 10% of the initial "spike" observed at short delay times. (The apparent relative weight of the slow component increases for longer excitation pulses.) Using a longer (160-fs) pulse, we were able to obtain better quality decay kinetics for $t > 1$ ps, which are shown separately in Figure 2b, for naphthalene-d_8^+. For all PAH cations, the slow kinetics can be fit using a single-exponential function with a time constant τ_s of a few picoseconds (e.g., Figures 1 and 2b). Both of the time constants, τ_f and τ_s, showed no variation with the concentration of the aromatic dopant, the extent of ionization by the 248-nm light, or the amount of water in the boric acid glass.

The overall kinetics (trace i in Figure 1) can be simulated by a convolution of the Gaussian response function (trace iii in Figure 1) with a biexponential function. Figures 1 and 3Sa

TABLE 2: Kinetic Parameters for PAH Cations in Boric Acid Glass

aromatic cation	band excited	τ_s at 295 K, ps[a]	τ_s at 15 K, ps[a]	τ_f, (fs)[b]
biphenyl$^+$	D_3	4.84 ± 0.12	7.1 ± 0.3	118 ± 8
		(*5.14* $\pm$ 0.16)	(*6.4* $\pm$ 0.16)	
naphthalene$^+$	D_2	8.2 ± 0.3	23 ± 1	190 ± 5
		(*6.6* $\pm$ 0.6)	(*18.8* $\pm$ 0.7)	
anthracene$^+$	D_2	10.2 ± 0.5	10.1 ± 0.2	[c]
		(*7.7* $\pm$ 0.14)	(*9.8* $\pm$ 0.2)	
perylene$^+$	D_5	18.8 ± 0.2	19.3 ± 0.2	[d]

[a] Lifetime for the slow component of the TG recovery kinetics for the perprotio D_0 state in boric acid. The lifetime for a perdeuterio species is in italics. The error limits indicate the standard deviation. [b] Lifetime for the fast component (the same for perprotio and perdeuterio species). [c] The fast component was not time-resolved. (This category also includes pyrene-h_{10}^+.) [d] The fast component is absent.

demonstrate a comparison between the kinetics obtained for radical cations of naphthalene-h_8 and -d_8. Although the time constant of the fast decay does not change with H/D substitution (Figure 1, traces i and ii and Figure 3Sa), the decay of the slow component for the perdeuterio cation is 1.24 times faster (Table 2). Cooling the sample also changes this slow component (Figure 2). For naphthalene-d_8^+, τ_s becomes progressively longer as the temperature decreases (Table 2), and the relative weight of the slow component increases by 50% upon cooling from 300 to 70 K (Figure 2b). Unlike the fast component, the slow decay kinetics are sensitive both to the sample temperature and H/D substitution in the aromatic radical cation.

Similar results were obtained for some other photoexcited PAH cations (Figures 4S, 5S, and 6S; the energetics are given in Table 1, and the lifetimes are given in Table 2). An increase in τ_s upon cooling from 295 to 15 K was observed for naphthalene-h_8^+ (increase of 2.8 times), biphenyl-h_{10}^+ (increase of 1.47 times, Figure 6S(a)), biphenyl-d_{10}^+ (1.25 times, Figure 6S(b)), and anthracene-d_{10}^+ (1.27 times, Figure 5S(b)). The only two exceptions are perylene-h_{12}^+ (Figure 7S) and anthracene-h_{10}^+ (Figure 5Sb), for which the change in τ_s with the temperature was negligible (Table 2). For anthracene$^+$, the relative weight of the slow component increased, and τ_s decreased upon H/D substitution (Figures 4Sa and 5Sb). The decrease in τ_s was higher at 295 K than at 15 K. For example, for anthracene$^+$ the kinetic isotope effect $\alpha_{H/D}$ defined as the ratio $\{\tau_s(h_{10})\}/\{\tau_s(d_{10})\}$ is 1.32 ± 0.09 at 295 K and 1.03 ± 0.04 at 15 K. For biphenyl$^+$, the isotope effect is reversed as compared to that of anthracene$^+$ and naphthalene$^+$: biphenyl-d_{10}^+ exhibits a *longer* τ_s than biphenyl-h_{10}^+, and the slow component has a *higher* relative weight in the perdeuterio cation (Figure 6S). Thus, only for biphenyl$^+$ does the decay rate of the slow component obey Siebrand's rule [10] for radiationless electronic transitions (which posits slower rates for D-substituted molecules with $\alpha_{H/D}$ of 0.75). As argued in the Discussion, this is due to the fact that the slow component is due to vibrational rather than electronic relaxation.

For anthracene -h_{10}^+ and -d_{10}^+, the fast component decays faster (<50 fs) than the time resolution of our TG spectrometer, and the time profile of the initial "spike" is close to that of the pump pulse (Figures 4Sa and 5Sa). For biphenyl -h_{10}^+ and -d_{10}^+, the fast component is clearly observed (Figure 4Sb), yielding $\tau_f = 118 \pm 8$ fs. As in naphthalene$^+$, the time constant τ_f of the fast component does not change upon H/D substitution (Figure 4). For these cations, the relative weight of the slow component correlates inversely with τ_f, increasing from anthracene$^+$ to biphenyl$^+$ to naphthalene$^+$ (Figures 1, 4S, and 5Sa).

Perylene$^+$ is different from other radical cations that we studied: the subpicosecond component is lacking, and the time constant of the slow component does not change from 15 to 295 K (Figure 7S). All picosecond kinetics are monoexponential and can be fit with a temperature-independent τ_s of ca. 18.8 ps (Figures 2a and 7S). This time is notably shorter than the value of 35 $\pm$ 3 ps obtained by Gumy and Vauthey [7] from a picosecond TG experiment on the same photosystem (532-nm, 25-ps fwhm pulse excitation). Our measurement is perhaps more accurate owing to the faster time resolution of our setup. Brodard et al.[8] reported a considerable temperature and isotope effect ($\alpha_{H/D}$ of ca. 1.23 at 295 K) on the decay rate of the TG signal for perylene$^+$ in sulfuric acid. Activation energies of 40 to 80 meV (300 to 350 K) that varied with the isotope composition of the dopant and the substrate were obtained (Table 2 in ref 8). We did not observe a temperature effect for perylene-h_{12}^+ in the boric acid glass (Figure 2).

4. Discussion

In our experiments, two relaxation regimes for the recovery kinetics of the D_0 state are observed: a subpicosecond regime and a picosecond regime. Given that these cations are photoexcited to their D_2, D_3, or even D_5 states, it is tempting to associate the fast component with a rapid (possibly, stepwise) $D_n \rightarrow D_1$ nonradiative transition and the slow component with a slower (also nonradiative) $D_1 \rightarrow D_0$ transition, by full analogy to the electronic deactivation in neutral PAH molecules.

For aromatic singlets, the slowest (usually radiative) transition is from their first excited S_1 states to their ground S_0 states (Kasha's rule), whereas less energetic $S_n \rightarrow S_{n-1}$ transitions are nonradiative and occur much faster (<10 ps). [9,10] Typically, the energy gaps between the S_n and S_{n-1} states are 2000 to 6000 cm^{-1} (vs 10 000−25 000 cm^{-1} for the S_1 and S_0 states), and the transition times are 10−20 fs to 1−5 ps (vs 1 ns to 1 μs for the S_1 and S_0 states). [9] For the doublet manifold of PAH cations, the energy gaps between the D_0 and D_1 states are 7000 to 10 000 cm^{-1} (Table 1), and one would expect to observe rapid nonradiative transitions in the doublet manifold. Though an approximate correlation between the energy gap and the corresponding relaxation rate exists (the energy gap law, see chapter 2.11 in ref 10), these rates can vary strongly between different photosystems, even if the energetics are similar (see, for example, Table 4 in ref 9). Generally, the energy-gap law is valid for relatively slow nonradiative transitions (such as $T_1 \rightarrow S_0$ and $S_1 \rightarrow T_1$ transitions); [10] for rapid transitions (such as $S_n \rightarrow S_{n-1}$ transitions), the law was shown to have limited applicability. [9]

A cursory examination of Tables 1 and 2 and Figures 2S and 8S suggests that τ_f and τ_s times obtained at 295 K do correlate with the D_n-D_1 and D_1-D_0 energy gaps, respectively (though no such correlation is apparent in the 15 K data). However, a detailed examination of the kinetics given in Appendix 1 in the Supporting Information indicates that the stepwise electronic relaxation is not supported by our results.

We suggest that the subpicosecond component observed for all PAH cations with the exception of perylene$^+$ corresponds to rapid internal $D_n \rightarrow D_0$ conversion in the doublet manifold, whereas the picosecond decay is due to VET from a hot D_0 state formed in the course of this rapid electronic relaxation (Figure 3). Such an interpretation readily accounts for the lack of isotope and temperature effects on the decay kinetics of the fast component. Because the rate of VET to the glass matrix depends on the matrix temperature and available vibrational modes in the donor, τ_s changes both with sample cooling and

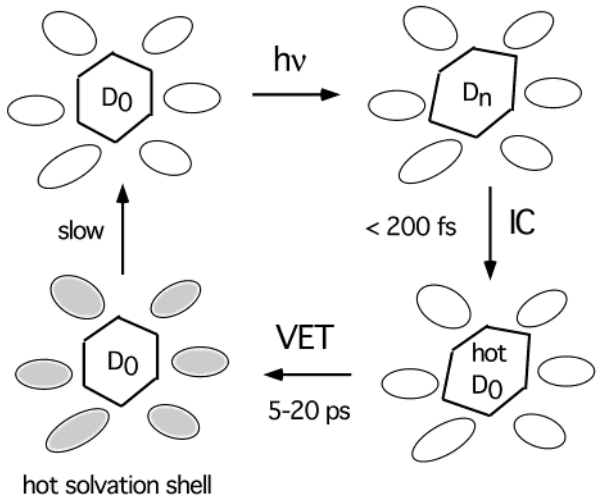

Figure 3. Scheme of the photophysical processes that contribute to the TG signal from a recovering ground D_0 state of an aromatic radical cation in a rigid matrix. Photoexcitation of the cation yields an excited D_n state that in <200 fs relaxes by internal conversion (IC) to a hot D_0 state; this process gives rise to the observed subpicosecond kinetics (fast component) that account for 70−95% of the total signal. Vibrational relaxation of the hot D_0 state, by vibrational energy transfer to the matrix (VET), occurs on the picosecond time scale and gives rise to the observed slow kinetics (a "tail" in Figure 1, trace i). These slow kinetics (unlike the rapid internal conversion) are temperature- and isotope-dependent. The heat transferred to the first solvation shell around the radical cation then slowly dissipates to the matrix bulk. The resulting density grating is not observed (<1 ns), because of the polarization geometry in our experiment.

H/D substitution in the PAH cation (see below). The decrease in the relative weight of the slow component at cryogenic temperatures is also rationalized: in a hot D_0 state, the spectral line is broader than the same line in a thermalized cation.[19a] For a given probe wavelength, the difference between the absorbances of the hot and relaxed D_0 states strongly depends on the overlap between the spectra of these two states: the greater the overlap, the smaller the slow TG signal. At the lower temperature, the line is narrower, the spectral overlap becomes worse, and the weight of the slow TG signal increases.

In perylene$^+$, because of an exceptionally large D_0-D_1 gap, the internal conversion is inhibited, and the 18.8-ps decay kinetics reflect the slow internal conversion of the D_1 state to the ground D_0 state. Because for perylene$^+$ (and possibly tetracene$^+$) [8] the slow component is due to electronic rather than vibrational relaxation, the contrast between temperature dependencies shown in Figure 2a is accounted for. Though our data are insufficient to establish the details of internal conversion in the doublet manifold, we believe that in all cases considered (with the exception of perylene$^+$) the fast component is from the $D_1 \rightarrow D_0$ transition; the relaxation of the higher D_n states to the D_1 state is so fast that it cannot be observed with our instrumentation.

Recently, Nishi and co-workers[20] studied the vibrational relaxation of naphthalene$^+$ and biphenyl$^+$ cations generated in the biphotonic ionization of their parent molecules in polar liquids (267-nm, 4-ps fwhm pulses were used for photoexcitation). Transient kinetics for Raman bands corresponding to interring C−C stretching modes were obtained. Both the Raman band centers and widths change on the picosecond time scale. For biphenyl$^+$ in 1-butanol, ethyl acetate, and acetonitrile, time constants of <5, 13, and 17 ps, respectively, for the thermalization of the C−C stretching bands were obtained. For naphthalene$^+$ and *trans*-stilbene$^+$ in acetonitrile, these time constants were 20−30 and 40 ps, respectively. Häupl et al.[21] studied the femtosecond dynamics of the photoexcited (D_1) radical cation of methyl viologen in acetonitrile and concluded that the electronic relaxation of the D_1 state occurred in <700 fs (<350 fs in water[22]). The resulting vibrationally excited D_0 state with a lifetime of 16 ps (2 ps in water[22]) had the same absorption spectrum as the parent cation but was shifted by 810 cm^{-1} to the red. This shift is equivalent to the frequency of the intra-ring C−C stretch. In addition to this "hot" D_0 state, there was another vibrationally excited D_0 state with a lifetime of 1 ps that was populated with the same rate as the long-lived state. These examples indicate that VET from PAH cations to the polar solvent typically occurs over 1−50 ps. Similar rates of VET to liquid solvent and solid host matrices (vibrational cooling) were observed for vibrationally excited PAH molecules in their S_0 and S_1 states.[19b]

The slow components observed in our TG experiments for naphthalene$^+$, biphenyl$^+$, and anthracene$^+$ have time constants between 5 and 10 ps (295 K) and 10−25 ps (15 K). These lifetimes are somewhat shorter than the typical lifetimes for vibrationally excited D_0 states in polar solvents (10−40 ps).[20,21] VET in a rigid matrix, such as boric acid glass, could be faster than in an organic liquid because the thermal conductivity of the glass is much higher (e.g., at 300 K, the thermal conductivity of vitreous boron trioxide is 3 times that of ethyl alcohol).[23] Besides, the initial stage of VET to the glass matrix may involve other than the high-frequency C−C stretching modes observed in the Raman experiments.[20] Nishi and co-workers suggest that the VET from a hot PAH cation to the matrix occurs not in one but two stages. The relatively slow rate of heat transfer observed in the time-resolved Raman experiments corresponds to cooling of the first solvation shell around the radical cation; this process is preceded by a faster VET from a hot radical cation to the first solvation shell. Because of insufficient time resolution, this fast process was not observed in the Raman experiments. This two-step mechanism has also been invoked to explain the vibrational relaxation of PAH molecules in transient absorption, grating, and Raman experiments of Sukowski et al. and others.[24]

The two-step mechanism qualitatively accounts for the isotope and temperature dependencies obtained in our TG experiments. The H/D isotope effect may originate through a VET that involves low-frequency C−H modes of a PAH cation[25] and vibrational modes of two glass-forming B_3O_6 rings that sandwich this planar cation between them (Appendix 2, Supporting Information). Such a process should not depend on the sample temperature. By contrast, cooling of the first solvation shell depends on the sample temperature, whereas it does not depend on the isotope composition of the dopant. In the two-step model, the overall kinetics for the picosecond component can be explained in the following way: When the temperature is low, the decay rate for the tail in the TG kinetics is limited by the (slow) rate of heat transfer to the glass bulk, and the isotope effect is negligible. At room temperature, the rate of heat transfer from the first solvation shell is comparable to the rate of VET from the hot D_0 state of the radical cation to the first solvation shell, and the decay kinetics of the TG signal exhibit isotope effects.

Implications for Photochemistry. Although PAH cations are photostable both in the gas phase and in the host media whose molecules have high ionization potentials (such as acetonitrile), in most matrices a hole injection[26,27] occurs: a photoexcited radical cation (Ar^+) oxidizes the solvent. This reaction occurs both in nonpolar liquids such as saturated hydrocarbons (where the resulting solvent radical cations is

metastable, reaction 1)[26] and in protic polar solvents (where the photoinduced charge transfer is concerted with proton transfer, reaction 2).[27]

$$Ar^{+\bullet} + RH \xrightarrow{h\nu} Ar + RH^{+\bullet} \quad (1)$$

$$Ar^{+\bullet} + ROH \xrightarrow{h\nu} Ar + RO^{\bullet} + ROH_2^{+} \quad (2)$$

The typical quantum yields for these two reactions are given in Table 1S in the Supporting Information. Because the heats of reactions 1 and 2 depend on the difference between the ionization potentials (IPs) of the parent aromatic molecule and the solvent, these quantum yields correlate with the molecular IP (Table 1S and refs 26 and 27). Interestingly, some PAH cations, such as anthracene$^+$ and biphenylene$^+$, exhibit very low yields of hole injection, though the corresponding IPs are sufficiently high and the absorbance of the cation at the excitation wavelength is strong.[27] Conversely, photoexcited perylene$^+$ oxidizes both polar and nonpolar solvents, though the corresponding reactions are barely exothermic.[26,27] Our kinetic data rationalize these observations. Photoexcited anthracene$^+$ is extremely short-lived, and the hole injection involving this species is inefficient. Photoexcited perylene$^+$ is very long-lived, and even slow, inefficient hole injection can occur. From the data of Tables 1S and 2, we estimate that for naphthalene$^+$ and biphenyl$^+$ in 2-propanol reaction 2 occurs with a rate constant of $(3-5) \times 10^{12}$ s^{-1}, whereas for perylene, this rate constant is just 10^8 s^{-1}. Note that if the lifetimes of the electronically excited radical cations involved in the "hole injection" were given by τ_s (as in the first model considered above) rather than by τ_f (as in the second model), then the anomalous behavior of anthracene$^+$ would be difficult to account for because this cation has a longer τ_s than naphthalene$^+$ and biphenyl$^+$ (Table 2).

Implications for Astrochemistry. Recently, Snow, Zukowski, and Massey[31] have undertaken an extensive study of the region surrounding the strong DIB line centered at 442.8 nm by surveying 35 young stars located in the Cyg OB2 association. They have found that the profile of this line is symmetric around the center, invariant across the sky, and can be well fit with a Lorentzian line whose width corresponds to the upper-state lifetime of 380 fs. Their estimate is within the same order of magnitude as the time constants for the rapid recovery of the D_0 states observed in our matrix isolation experiments. Thus, our observations strengthen the link between the DIB lines and PAH cations. In another recent study, Biennier, Salama, Allamandola, and Scherer[32] have used pulsed discharge nozzle cavity ring-down spectroscopy to study the photophysics of cold, gas-phase PAH cations. For the same D_2 band of naphthalene$^+$ studied in this work, they obtained a lifetime of 210 fs (vs 190 $\pm$ 5 fs obtained in our experiments). This result suggests that the lifetimes of electronically excited states in the gas-phase and matrix-isolated PAH cations are comparable.

5. Concluding Remarks

Femto- and picosecond transient grating kinetics for matrix-isolated photoexcited PAH cations can be understood in terms of two processes (Figure 3): (i) a very rapid (<200 fs) internal conversion to a hot D_0 state and (ii) a vibrational energy transfer from this state to the solid matrix (4−25 ps). A two-step mechanism[20] for VET from the hot D_0 state to the glass matrix is suggested. The ultrafast internal conversion accounts for the remarkable stability of PAH cations toward vis and near-UV photoexcitation.

Given the high rates of electronic deactivation and hole injection for aromatic radical cations, we conclude that (with few exceptions) the participation of electronically excited PAH cations in exothermic electron-transfer reactions[28] is unlikely. Even if hole injection[26,27] does not occur, the excited PAH cations rapidly deactivate in less than 1 ps. However, both our TG results and other recent studies[20−22] suggest that the vibrational cooling of organic radical cations is relatively slow. This cooling can occur on the same time scale as charge recombination, and the formation of vibrationally excited cations, whose reaction properties can be different from those of the ground-state cations, should be taken into account.

Acknowledgment. This work was performed under the auspices of the Office of Science, Division of Chemical Science, U.S. DOE under contract number W-31-109-ENG-38. I.A.S. thanks Dr. F. Salama and Professors T. P. Snow, T. Oka, and V. M. Bierbaum for helpful discussions and Dr. M. C. Sauer, Jr. for technical assistance. S.P. acknowledges the support of the DGA through the contract number DSP/01-60-056.

Supporting Information Available: Two-step electronic relaxation scenario rebuffed. Intermolecular VET in boric acid glass. Additional references. Quantum yields for 532-nm photon-induced "hole injection" in room-temperature *trans*-decalin and 2-propanol. This material is available free of charge via the Internet at http://pubs.acs.org.

References and Notes

(1) Snow, T. P. *Spectrochim. Acta, Part A* **2001**, *57*, 615 and references therein.

(2) Allamandola, L. J.; Tielens, A. G. G. M.; Barker, J. R. *Ap. JS* **1989**, *71*, 733. Salama, F.; Galazutdinov, G. A.; Krelowski, J.; Allamandola, L. J.; Musaev, F. A. *Ap. J.* **1999**, *526*, 265. For matrix isolation UV−vis spectroscopy of D_{2h}-symmetric PAH cations see, for example, Vala, M.; Szszepanski, J.; Pauzat, F.; Parisel, O.; Talbi, D.; Ellinger, Y. *J. Phys. Chem.* **1994**, *98*, 9187; Vala, M.; Szszepanski, J.; Pauzat, F.; Parisel, O.; Talbi, D.; Ellinger, Y. *J. Chem. Phys.* **1993**, *98*, 4494; and pp 717−815 in the special issue of *Spectrochim. Acta, Part A* **2001**, *57*, No. 14 and references therein.

(3) Le Page, V.; Snow, T. P.; Bierbaum, V. M. *Ap. J. S.* **2001**, *132*, 233. Snow, T. P.; Le Page, V.; Keheyan, Y.; Bierbaum, V. M. *Nature* **1998**, *391*, 259. Snow, T. P.; Le Page, V.; Keheyan, Y.; Bierbaum, V. M. *J. Am. Chem. Soc.* **1999**, *121*, 9435.

(4) Bohme, D. K. *Chem. Rev.* **1992**, *92*, 1487 and references therein.

(5) Gotkis, Y.; Oleinikova, M.; Naor, M.; Lifshitz, C. *J. Phys. Chem.* **1993**, *97*, 12282. Ho, Y.-P.; Dunbar, R. C.; Lifshitz, C. *J. Am. Chem. Soc.* **1995**, *117*, 6504. Ling, Y.; Lifshitz, C. *J. Mass Spectrosc.* **1997**, *32*, 1219. Jochims, H. W.; Baumgärtel, H.; Leach, S. *Ap. J.* **1999**, *512*, 500.

(6) Haselbach, E.; Bally, T. *Pure Appl. Chem.* **1984**, *56*, 1203. Miller, T. *Annu. Rev. Phys. Chem.* **1982**, *33*, 257.

(7) Gumy, J.-C.; Vauthey, E. *J. Phys. Chem. A* **1997**, *101*, 8575.

(8) Brodard, P.; Sarbach, A.; Gumy, J.-C.; Bally, T.; Vauthey, E. *J. Phys. Chem. A* **2001**, *105*, 6594.

(9) Ermolaev, V. L. *Russ. Chem. Rev.* **2001**, *70*, 471 (Engl. transl.)

(10) Medvedev, E. S.; Osherov, V. I. *Radiationless Transitions in Polyatomic Molecules*; Springer-Verlag: New York, 1995.

(11) For the photophysics of light- and radiation-induced ionization of PAH molecules trapped in boric acid glass, see (in chronological order) Bennema, P.; Hoijtink, G. J.; Lupinski, J. H.; Oosterhoff, L. J.; Selier, P.; van Voorst, J. D. W. *Mol. Phys.* **1959**, *2*, 431. Vincow, G.; Johnson, P. M. *J. Chem. Phys.* **1963**, *39*, 1143. Hughes, F.; Kirk, R. D.; Patten, F. W. *J. Phys. Chem.* **1964**, *40*, 872. Lesclaux, R.; Joussot-Dubien, J. *J. Chim. Phys.* **1968**, *65*, 1313. Treinin, A. In *Radical Ions*; Kaiser, E. T., Kevan, L., Eds.; Wiley: London, 1968; p 525. Owen, G. S.; Vincow, G. *J. Chem. Phys.* **1971**, *54*, 368. Lesclaux, R.; Joussot-Dubien, J. In *Organic Molecular Photophysics*; Birks, J. B., Ed.; Wiley: London, 1973; Vol 1, p 457. Ewald, M.; Leslaux, R. *Int. J. Radiat. Phys. Chem.* **1976**, *8*, 679. Andreev, O. M.; Smirnov, V. A.; Alfimov, M. V. *J. Photochem.* **1977**, *7*, 149. Joussot-Dubien, J.; Lamotte, M.; Pereyre, J. *J. Photochem.* **1981**, *17*, 347. Khan, Z. H. *Can. J. Spectrosc.* **1984**, *29*, 63 and references therein.

(12) Shida, T.; Hamill, W. H. *J. Chem. Phys.* **1966**, *44*, 2375. Shida, T.; Iwata, S. *J. Am. Chem. Soc.* **1973**, *95*, 3473. Shida, T. *Electronic Absorption Spectra of Radical Ions*; Elsevier: Amsterdam, 1988.

(13) The temperature values given in this work are for the cryostat rather than the sample temperatures. Because of the poor thermal conductivity of the boric acid glass, local heating of the irradiated zone can be important, especially at very low temperature. Assuming that 1 mW of energy is absorbed in a 50-μm diameter-spot in a 2-mm-diameter, 300-μm-thick glass disc (attached to the cryostat finger at the rim), we estimate that the actual temperature in the irradiated zone is 4 K higher at 300 and 24 K higher at 15 K as compared to the cryostat temperature.

(14) Fayer, M. D. *Annu. Rev. Phys. Chem.* **1982**, *33*, 63. Deeg, F. W.; Fayer, M. D. *J. Chem. Phys.* **1989**, *91*, 2269.

(15) Shkrob, I. A.; Crowell, R. *Phys. Rev. B* **1998**, *57*, 12207.

(16) Negri, F.; Zgierski, M. Z. *J. Chem. Phys.* **1994**, *100*, 1387. For more recent ab initio and density functional calculations, see Hirata, S.; Lee, T. J.; Head-Gordon, M. *J. Chem. Phys.* **1999**, *111*, 8904 and refs 19, 32, and 33 therein.

(17) (a) Eland, J. H. D.; Danby, C. J. *Z. Naturforsch., A* **1968**, *23*, 355. (b) Ruscic, B.; Kovac, B.; Klasinc, L.; Güsten, H. *Z. Naturforsch., A* **1978**, *33*, 1006. (c) Andrews, L.; Arlinghaus, R. T.; Payne, C. K. *J. Chem. Soc., Faraday Trans. 2* **1983**, *79*, 885. Buntinx, G.; Poizat, O. *J. Chem. Phys.* **1989**, *91*, 2153. (d) Puiu, A. C.; Andrews, L.; Chupka, W. A.; Colson, S. D. *J. Chem. Phys.* **1982**, *76*, 3854. (e) Heidenreich, A.; Münzel, N.; Schweig, A. *Z. Naturforsch., A* **1986**, *41*, 1415.

(18) (a) Szczepanski, J.; Drawdy, J.; Wehlburg, C.; Vala, M. *Chem. Phys. Lett.* **1995**, *245*, 539. (b) Khan, Z. H. *Can. J. Spectrosc.* **1978**, *23*, 8.

(19) (a) Amirav, A.; Even, U.; Jortner, J. *J. Phys. Chem.* **1982**, *86*, 3345. Lenz, K.; Pfeiffer, M.; Lau, A.; Elasesser, T. *Chem. Phys. Lett.* **1994**, *229*, 340. Chudoba, C.; Riedle, E.; Pfeiffer, M.; Elasesser, T. *Chem. Phys. Lett.* **1996**, *263*, 622. Fournier, T.; Pommeret, S.; Mialocq, J.-C.; Deflandre, A.; Rozot, R. *Chem. Phys. Lett.* **2000**, *325*, 171. (b) For example, Emmerling, F.; Lettenberger, M.; Lauberau, A. *J. Phys. Chem.* **1996**, *100*, 19251. Hill, J. R.; Chronister, E. L.; Chang, T. C.; Kim, H.; Postlewaite, J. C.; Dlott, D. D. *J. Chem. Phys.* **1988**, *88*, 949 and references therein. Foggi, P.; Pettini, L.; Santa, I.; Righini, R.; Califano, S. *J. Phys. Chem.* **1995**, *99*, 7439. Baier, J.; Posch, P.; Jungmann, G.; Schmidt, H.-W.; Seilmeier, A. *J. Chem. Phys.* **2001**, *114*, 6739. Jiang, Y.; Blanchard, G. J. *J. Phys. Chem.* **1994**, *98*, 9411. Hambir, S. A.; Jiang, Y.; Blanchard, G. J. *J. Chem. Phys.* **1993**, *98*, 6075.

(20) Nakabayashi, T.; Kamo, S.; Watanabe, K.; Sakuragi, H.; Nishi, N. *Chem. Phys. Lett.* **2002**, *355*, 241. Nakabayashi, T.; Kamo, S.; Sakuragi, H.; Nishi, N. *J. Phys. Chem. A* **2001**, *105*, 8605.

(21) Häupl, T.; Lomoth, R.; Hammerström, L. *J. Phys. Chem. A* **2003**, *107*, 435.

(22) Huang, Y.; Hopkins, J. B. *J. Phys. Chem.* **1996**, *100*, 9585.

(23) Leadbetter, A. J.; Jeapes, A. P.; Waterfield, C. G.; Maynard, R. *J. Phys. (Paris)* **1977**, *38*, 95. Nilsson, O.; Sandberg, O.; Bäckström, G. *Int. J. Thermophys.* **1985**, *6*, 267.

(24) Sukowski, U.; Seilmeier, A.; Elsaesser, T.; Fischer, S. F. *J. Chem. Phys.* **1990**, *93*, 4094. Schwartzer, D.; Troe, J.; Votsmeier, M.; Zerezke, M. *J. Chem. Phys.* **1996**, *105*, 3121. Iwata, K.; Hamaguchi, H. *J. Phys. Chem. A* **1997**, *101*, 632. Okazaki, T.; Hirota, N.; Terazima, M. *J. Chem. Phys.* **1999**, *110*, 11399.

(25) Bakes, E. L. O.; Tielens, A. G. G. M.; Bauschlicher, C. W., Jr. *Ap. J.* **2001**, *556*, 501. Salama, F.; Allamandola, L. J. *J. Chem. Phys.* **1991**, *94*, 6964.

(26) Shkrob, I. A.; Sauer, M. C., Jr.; Trifunac, A. D. *J. Phys. Chem. B* **1999**, *103*, 4773.

(27) Shkrob, I. A.; Sauer, M. C., Jr.; Liu, A. D.; Crowell, R. A.; Trifunac, A. D. *J. Phys. Chem. A* **1998**, *26*, 4976.

(28) Mataga, N.; Kanda, Y.; Tsuyoshi, A.; Miyasaka, H.; Okada, T.; Kakitani, T. *Chem. Phys.* **1988**, *127*, 239.

(29) Vala, M.; Szczepanski, J.; Pauzat, F.; Parisel, O.; Talbi, D.; Ellinger, Y. *J. Phys. Chem.* **1994**, *98*, 9187.

(30) Schmidt, W. *J. Chem. Phys.* **1977**, *66*, 828.

(31) Snow, T. P.; Zukowski, D.; Massey, P. *Ap. J.* **2002**, *578*, 877.

(32) Biennier, L.; Salama, F.; Allamandola, L.; Scherer, J. *J. Chem. Phys.* **2002**, *118*, 7863.